Neurological Sciences (2019) 40:1255–1265
https://doi.org/10.1007/s10072-019-03783-w

ORIGINAL ARTICLE

Abnormal nuclear aggregation and myotube degeneration in myotonic dystrophy type 1

Yanlin Wang[1] · Lei Hao[2] · Hui Li[3] · John D. Cleary[4] · Michael P. Tomac[5] · Arjun Thapa[5] · Xiuming Guo[6] · Desmond Zeng[3] · Hongcai Wang[5] · MacKezie McRae[5] · Olivia Jastrzemski[5] · Ali Marichen Smith-Fassler[5] · Yuming Xu[1] · Guangbin Xia[5]

Received: 13 February 2018 / Accepted: 20 February 2019 / Published online: 19 March 2019

Abstract

Myotonic dystrophy type 1 (DM1) is caused by CTG nucleotide repeat expansions in the 3′-untranslated region (3′-UTR) of the dystrophia myotonica protein kinase (*DMPK*) gene. The expanded CTG repeats encode toxic CUG RNAs that cause disease, largely through RNA gain-of-function. DM1 is a fatal disease characterized by progressive muscle wasting, which has no cure. Regenerative medicine has emerged as a promising therapeutic modality for DM1, especially with the advancement of induced pluripotent stem (iPS) cell technology and therapeutic genome editing. However, there is an unmet need to identify in vitro outcome measures to demonstrate the therapeutic effects prior to in vivo clinical trials. In this study, we examined the muscle regeneration (myotube formation) in normal and DM1 myoblasts in vitro to establish outcome measures for therapeutic monitoring. We found normal proliferation of DM1 myoblasts, but abnormal nuclear aggregation during the early stage myotube formation, as well as myotube degeneration during the late stage of myotube formation. We concluded that early abnormal nuclear aggregation and late myotube degeneration offer easy and sensitive outcome measures to monitor therapeutic effects in vitro.

Keywords Myotonic dystrophy · Nuclear · Aggregation · Myotube · Foci · Degeneration

Introduction

Myotonic dystrophy (dystrophia myotonica, DM) Type 1 (DM1) is a dominant monogenic neurodegenerative disorder. DM1is the most common form of muscular dystrophy in adults with the prevalence of 8–10/100,000 [1, 2]. Its congenital form, known as congenital myotonic dystrophy (CDM), is reported to have an incidence of 2.1 per 100,000 live births [3]. The disease is caused by an unstable CTG nucleotide repeat expansion (> 50 CTG repeats) within the 3′-untranslated region (3′-UTR) of the dystrophia myotonica protein kinase (*DMPK*) gene on chromosome 19q13.3 [4]. The expanded repeats encode for toxic CUG RNA repeats, which aggregate with splicing factors to form intranuclear RNA foci, a molecular hallmark of DM1. The sequestration of splicing factors causes aberrant splicing of transcripts in a large number of genes (see recent reviews) [2, 5–10]. These aberrant splicing events account for the clinical presentation of myotonia, muscle weakness, diabetes, cardiac events, and cognitive impairment. Unfortunately, there is no cure for the disease.

Induced pluripotent stem (iPS) cell technology has emerged as a potential avenue for regenerative medicine,

Electronic supplementary material The online version of this article (https://doi.org/10.1007/s10072-019-03783-w) contains supplementary material, which is available to authorized users.

✉ Yuming Xu
xuyuming@zzu.edu.cn

✉ Guangbin Xia
guxia@salud.unm.edu; guangbin.xia@gmail.com

[1] Department of Neurology, The First Affiliated Hospital of Zhengzhou University, Henan 450000, China

[2] Department of Neurology, The Fifth People's Hospital of Chongqing, Chongqing 400062, China

[3] Department of Neurology, University of Florida, Gainesville, FL, USA

[4] Department of Molecular Genetics and Microbiology, University of Florida, Gainesville, FL, USA

[5] Department of Neurology and Neuroscience, School of Medicine, University of New Mexico, Albuquerque, NM 87131, USA

[6] Department of Neurology, The First Affiliated Hospital of Chongqing Medical University, Chongqing 400016, China

which includes personalized cell replacement therapy [11–13]. Protocols have been developed to differentiate iPS cells into skeletal muscle progenitors [14–17] and we have developed a strategy to correct the mutation in DM 1 iPS cells [18, 19]. However, there is an unmet need to find in vitro outcome measures to assess therapeutic effects. In vitro myotube formation assays are widely used in evaluating myogenesis or muscle regeneration in muscular dystrophies [20]. However, there are several inconsistent reports about DM1 myotube formation [21–27]. Many factors may explain the contradictory/inconsistent findings, including differences in the study subjects (age, sex, age at onset, the number of CTG repeats), the clinical course, the site and severity of the muscle from which satellites were isolated, and the passage number of the myoblasts used in the assay, as well as the time point of observation of myotube formation. In the present study, we used early passage myoblasts to investigate the process of myotube formation longitudinally, from myoblast proliferation to early and late myotube formation. Our aim was to establish outcome measures in an in vitro culture system for monitoring DM1 therapies.

Materials and methods

Reagents

FISH probes were HPLC-purified, Cy3-labeled $(CAG)_{10}$ synthesized by Integrated DNA Technologies (Coralville, IA). Antibodies: Desmin (Thermo Fisher, Cat. no. RB-9014), myosin heavy chain (MHC) (Sigma, Cat. no. M1570), alpha-tubulin (Sigma, Cat. no. M1570), Aurora B (Cell Signaling, Cat. no. 2914S), MBNL1 (3A4) (Santa Cruz, Cat. no. sc-47740), or MBNL2 (3B4) (Santa Cruz, Cat. no. sc-136167).

IRB approval and myoblast isolation and maintenance

Adult-onset DM1 subjects were recruited. The clinical data of the research subjects have been described previously and the Southern blot of the fibroblasts from the subjects confirmed the expansion of CTG repeats to be approximately 2829–3575 repeats for DM1-03 and 1933–3152 repeats for DM1-05 [28]. Muscle biopsies were performed using a 7G UCH muscle biopsy needle (Cat. no. 8066, Web: www.cadencescience.com) in the vastus lateralis. Samples were cut into about 15 pieces and seeded into a 6-cm dish and myoblasts were expanded at a 1:2 ratio until passage 4, when the cells grew to 80% confluence in two 75-cm^2 flasks as it took about 2 weeks, for DM-03 and normal, and 4 weeks, for DM-05, to get the same number of cells. All the following experiments were conducted within passage 7, with synchronized passages of each cell line.

Cell culture

Permissive myoblast growth media (Clonetics™ SkGM™ BulletKit™ (CC-3160) containing a basal medium and growth supplements (human epidermal growth factor; fetuin; bovine serum albumin, dexamethasone; insulin, and gentamicin/amphotericin-B) were obtained from Lonza Walkersville, Inc. (Walkersville, MD). The non-permissive skeletal muscle differentiation medium was DMEM/F12 50:50 supplemented with 2% horse serum (Thermo Fisher Scientific, Cat. no. 16050122).

RT-PCR for alternative splicing assay

Total RNA was isolated using Quick-RNA MiniPrep (Zymo Research, Irvine, CA, Cat. no. R1055,) according to the manufacturer's protocol. Reverse transcription, PCRs, and alternative splicing assays were performed as described previously [18, 29]. Primers for BIN 1 are BIN1-F: 5′-AGAA CCTCAATGATGTGCTGG 3'and BIN1-R: 5′-TCGT GGTTGACTCTGATCTCGG-3′.

Cell proliferation assay

2×10^3 myoblasts (passage 5) per well were plated in 100-μl media in a 96-well plate (8 eight wells for each cell). A WST-1 cell proliferation colorimetric assay was performed on days 0, 1, and 5 before cells became confluent using a kit from Roche (Cat. no. 11644807001, Mannheim, Germany). Day 0 was measured 6 h after plating the cells. 10 μl of WST-1 working solution was added to 100 μl of culture medium for each well, followed by incubation of 2.4 h at 37 °C. The plate was then read for absorbance at a wavelength of 450 nm.

Myotube formation and nuclear aggregation assay

Myoblasts were grown in a 5% CO_2 humidified incubator. Myoblasts were detached with 0.05% trypsin and resuspended in a permissive culture medium. 3×10^4 cells were plated per chamber in ibidiTreat μ-slides (2.5×10^4 cells/cm^2) supplemented with 80 μl media an hour later after the cells attached. The cells in the chamber were allowed to grow or another 12 h until the myoblasts were about 80% confluent. The medium was changed to a non-permissive medium every day for 3, 5, or 10 days as indicated. Cells were then subjected to RNA FISH and immunostained with MHC (slow) as described below.

Myotube formation was evaluated either by the myotube formation index (the percentage of nuclei in myosin-positive myotubes over a total number of nuclei; a total of 30 fields were counted in three representative regions of the ibidiTreat chamber at × 400 magnification) or by average myotube number per × 200 magnification field (30 fields were counted in

three representative regions of the ibidiTreat chamber). Nuclear aggregation was assessed by the nuclear aggregation index (the percentage of myotubes with nuclei aggregation, defined by more than three misaligned, eccentric nuclei at the end of the myotube).

FISH and immunofluorescence staining

FISH was performed as described previously [28, 30]. Briefly, cells were fixed in 10% buffered formalin phosphate, and then dehydrated in pre-chilled 70% ethanol. Cells were then hybridized with Cy3-labeled $(CAG)_{10}$ DNA probes (500 pg/μl) after pre-treatment. After hybridization, cells were washed three times in pre-warmed 40% formamide, 2× SCC buffer for 30 min at 37 °C and once in PBS (pH 7.4) followed by IF staining. Cells were incubated overnight at 4 °C with antibodies against Desmin (1:100), MHC (1:400), alpha-tubulin (1:1000), Aurora B (1:100) or MBNL1/2 (1:100). The following day, slides were washed and incubated with the secondary antibody conjugated with Alexa Fluor 488 (Invitrogen) (1:500) for 30 min at room temperature. Finally, the slides were washed with PBS and mounted with Vectashield mounting medium containing DAPI. Photomicrographs were taken using Olympus IX81-DSU Spinning Disk confocal microscope. Confocal images were captured in a *z*-stack interval of 0.5-μm increments, using a 60X objective to quantify the foci within the cellular volume. Mitotic phases were identified by mitotic spindle and chromosome morphologies.

Statistical analysis

An ANOVA run on SPSS software was used to compare the difference among groups. $P < 0.05$ was used as significant difference.

Results

Equal percentage of Desmin-positive myoblasts from normal and DM1 subjects

Myoblasts that had been egressed from muscle tissues of one normal and two DM1 (DM-03, DM-05) subjects were expanded in permissive myoblast culture medium. To estimate the percentage of myogenic cells, we performed an immunocytochemistry analysis using a muscle-specific anti-Desmin antibody. We found no significant difference in percentage of Desmin-positive cells among the three myoblast lines (Fig. 1a–d, Supplemental Fig. 1). All three cell lines had relatively pure myoblasts with Desmin-positive cells above 90% at passage 7. In the medium permissive for proliferation, DM1 myoblasts were spindle shaped and there was no morphology

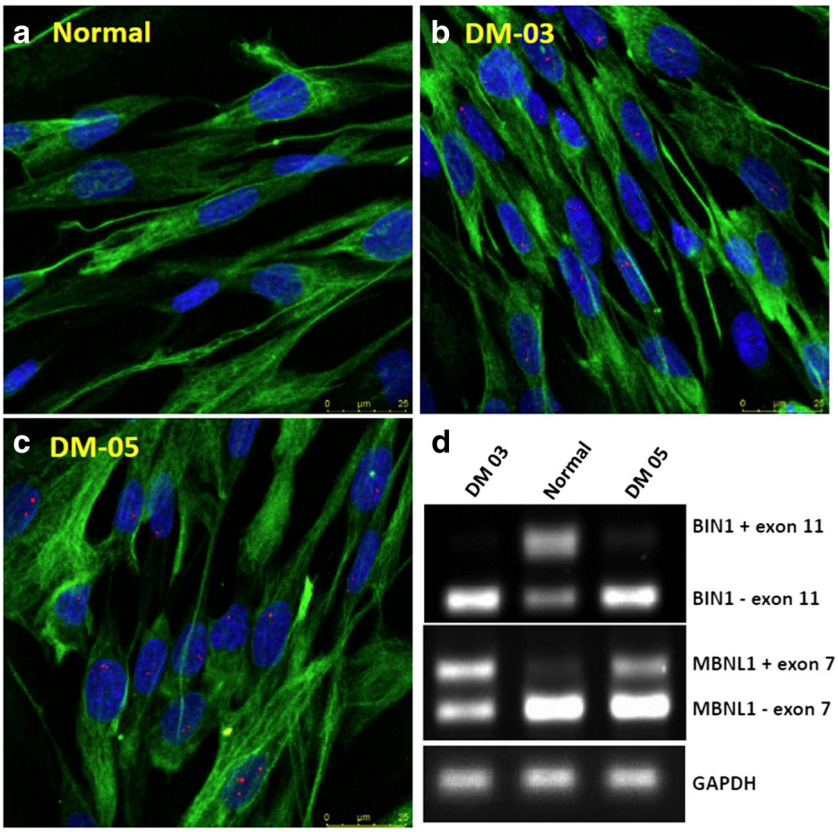

Fig. 1 All three myoblast lines had similar percentage of Desmin-positive myoblasts (green). There was no difference between normal and DM1 cells. DM1 myoblasts (DM-03 and DM-05) showed intranuclear foci (red)

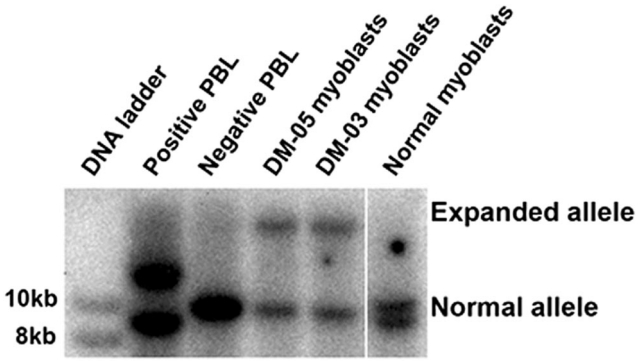

Fig. 2 Southern blot of normal and DM1 myoblasts. Genomic DNAs were digested by EcoRI, which will generate two different normal allele size, one around 8.7 kb and one around 9.6 kb (Alu− or Alu+ in intron 8 polymorphisms). Normal myoblasts in this study contain both alleles. CTG repeats in DM-03 and DM-05 myoblasts are calculated to be around 3600. Negative and positive peripheral blood (PBL) samples are included as controls

difference from the normal control. Alternative splicing assay confirmed the aberrant splicing of exon 11 of BIN1 gene in the DM1 myoblasts (Fig. 1e). The CTG expansion was confirmed by Southern blot (Fig. 2).

Increased proliferation of DM1 myoblasts

In order to investigate the proliferative function of DM1 myoblasts, we performed morphological analysis of mitosis by immunofluorescence and cell proliferation assays. Aurora B is a protein kinase and a chromosomal passenger protein that undergoes dynamic redistribution during mitosis [31]. Therefore, we performed Aurora B staining to investigate the mitosis process in myoblasts. We found Aurora B follows the normal distribution dynamics. In both normal and DM1 myoblasts, Aurora B was found at centromeres in the prophase and in the metaphase (Fig. 3a). It then relocated to midzone microtubules in the anaphase (Fig. 3b), and subsequently condensed and coalesced laterally (Fig. 3c) to form the midbody during cytokinesis (Fig. 3d). Tubulin staining also confirmed normal morphology during mitosis (Fig. 3). Aurora B labeling was further analyzed to quantify proliferative capability, and showed higher percentage of DM1 myoblasts undergoing mitosis compared to normal myoblasts (Fig. 4a). Cell proliferation capacity was further quantified by WST-1 cell proliferation assay, and again showed the higher proliferative rate in DM1 myoblasts (Fig. 4b).

Accumulation of nuclear foci during early myotube formation

Although DM1 is a multisystem disorder, muscle tissue is primarily affected. One possible explanation is the relatively high expression of the *DMPK* gene in muscles and, accordingly, more toxic intranuclear mutant transcripts. Intranuclear RNA foci have been shown to be toxic to the cell via a RNA gain-of-function of expanded CUG repeats [2, 5–10]. We have shown that intranuclear RNA foci undergo dynamic changes in proliferating cells [30]. Intranuclear RNA foci are released into the cytoplasm and degraded during mitosis, which offers a mechanism to lessen the toxic nuclear RNA load [30]. Since myoblasts from DM1 did not demonstrate any obvious morphological abnormality, we further investigated whether this was due to the low expression of DMPK in myoblasts compared to differentiated muscle cells. We observed a higher number and a bigger size of intranuclear RNA foci in DM1 myotubes compared to myoblasts (quantitative data not

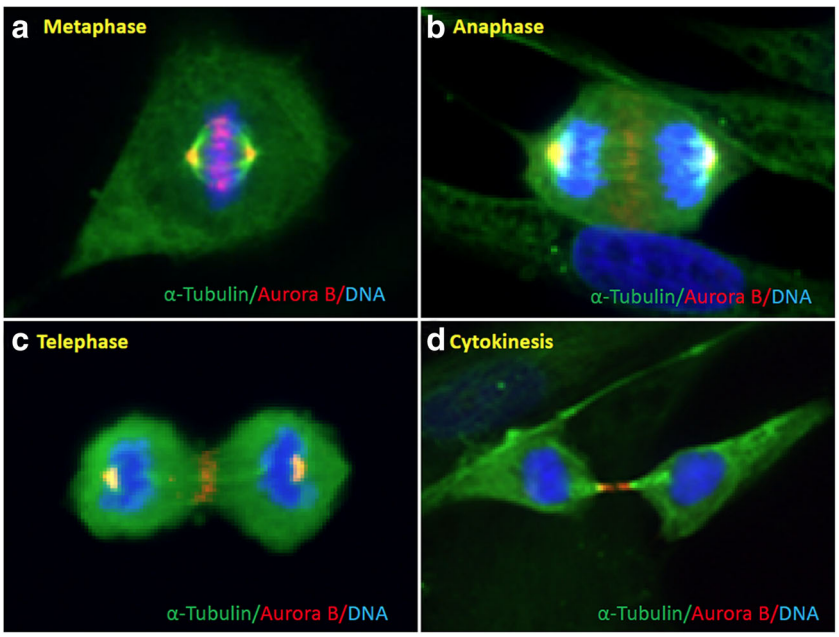

Fig. 3 Dynamics of Aurora B (red) during mitosis of DM1 myoblasts. Aurora B localized to the centromeres at the metaphase (**a**) and persisted through the anaphase (**b**), but relocated to the midzone microtubules. At the telephase (**c**) and cytokinesis (**d**), Aurora B condensed and coalesced laterally to form the midbody before abscission. Cell morphology was shown by α-tubulin staining (green)

shown). We also found more foci in myotubes than non-myotube-forming cells (Fig. 5 b, c, and d). These results suggest that intranuclear RNA foci accumulate during muscle differentiation. We further studied the co-localization of intranuclear RNA foci and MBNL1. We found that intranuclear RNA foci and MBNL1 co-localization occurs in myoblasts. We also observed that co-localization depleted the soluble MBNL1 as compared to normal myoblasts (Fig. 6). These findings confirm that the sequestration of MBNL1 contributed to the pathogenesis in DM1.

Abnormal nuclear aggregation during early stage of myotube formation in DM1

Sequential images of cultured myoblasts were acquired during myotube formation. We observed that nuclei started accumulating as early as day 2 in DM1 myoblasts, and aggregates commenced (more than three misaligned, eccentric nuclei at the end of myotubes) on day 3 in DM1 myoblasts (Fig. 7, Supplemental Fig. 2).

On day 5, aggregation became more prominent, and tended to accumulate at the ends of newly formed myotubes, showing decreased nuclear anisotropy (Fig. 8 a, b). In contrast, the fusion started later in normal myoblasts (not obvious on day 2), and the nuclei were aligned linearly and more evenly distributed along the myotubes with well-organized sarcomeres (Fig. 8 c). To quantify this phenomenon, we established a nuclear aggregation index (percentage of myotubes with aggregation of nuclei). We found significantly greater nuclear aggregation in DM1 myoblasts compared to the normal control (Fig. 8 d).

On day 5 of the differentiation, we again noted that the foci became even more prominent in the aggregated nuclei and they co-localized with MBNL1, leading to the depletion of soluble MBNL1 in the nuclei compared to the normal control (Fig. 9). We concluded that nuclear aggregation index may be used as an early outcome measure to reflect the defective myotube formation in DM1 and to assess the effects of potential therapies.

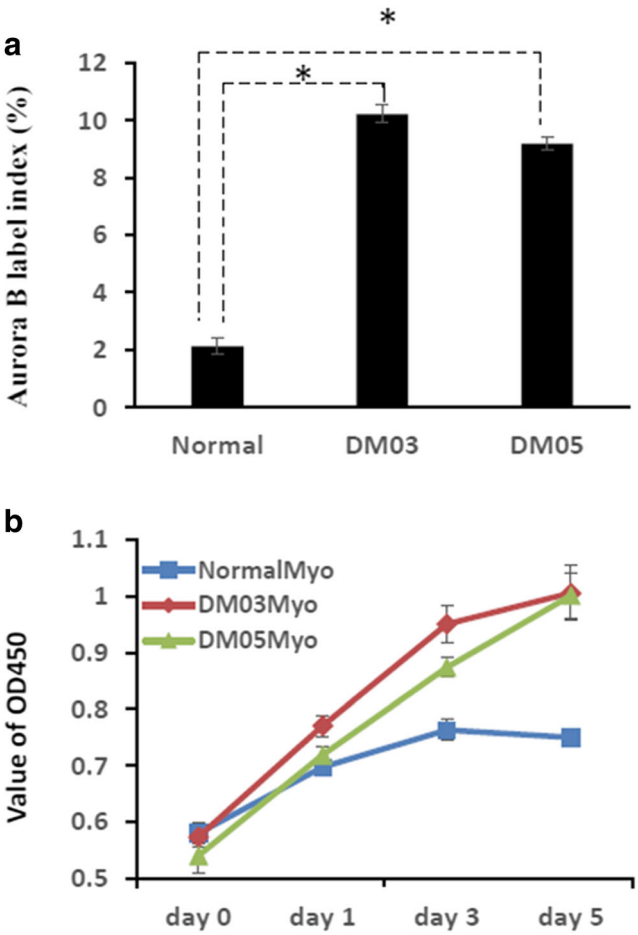

Fig. 4 DM1 myoblasts have a higher proliferation rate than normal. **a** Aurora B labeling index to reflect cell proliferative capacity. Aurora B labeling index was calculated as the percentage of Aurora B-positive cells that are undergoing mitosis (from prophase to cytokinesis). Both DM1 myoblasts (DM03 and DM05) have higher Aurora B labeling (*$P < 0.01$). **b** Cell proliferation was evaluated by a WST-1 cell proliferation colorimetric assay

Myotube degeneration during the late stage of myotube formation in DM1

To measure dynamic changes of myotube development, we observed myotube formation over sequential days in DM-03 myoblasts and compared them to normal myoblasts. We noted that myotubes formed earlier in DM1 cells than in the normal controls, but looked comparable to normal myotubes on day 5 of the differentiation. Significant degeneration of myotubes only happened on day 10 of the differentiation (Fig. 10). To verify whether the lower myotube fusion index in DM1 was due to unequal cell number, we performed a separate experiment on the both DM-03 and DM-05 myoblasts and confirmed the higher level of myotube degeneration on day 10, but without significant difference in nuclei density. This suggests that myotube degeneration precedes cell loss (Fig. 11).

Discussion

Satellite cells play an important role in adult myogenesis. After asymmetric division, the apical satellite cell undergoes multiple rounds of division to generate muscle precursor cells (myoblasts) prior to fusion into multinucleated myofibers [32]. Though it is relatively challenging to study satellite cells in vitro, the abnormalities of satellite cells in muscular dystrophy have recently been found in Duchenne muscular dystrophy [33]. In this study, we focused our study on early myogenesis from satellite-derived myoblasts, where we found no proliferative dysfunction of DM1 myoblasts. Previous

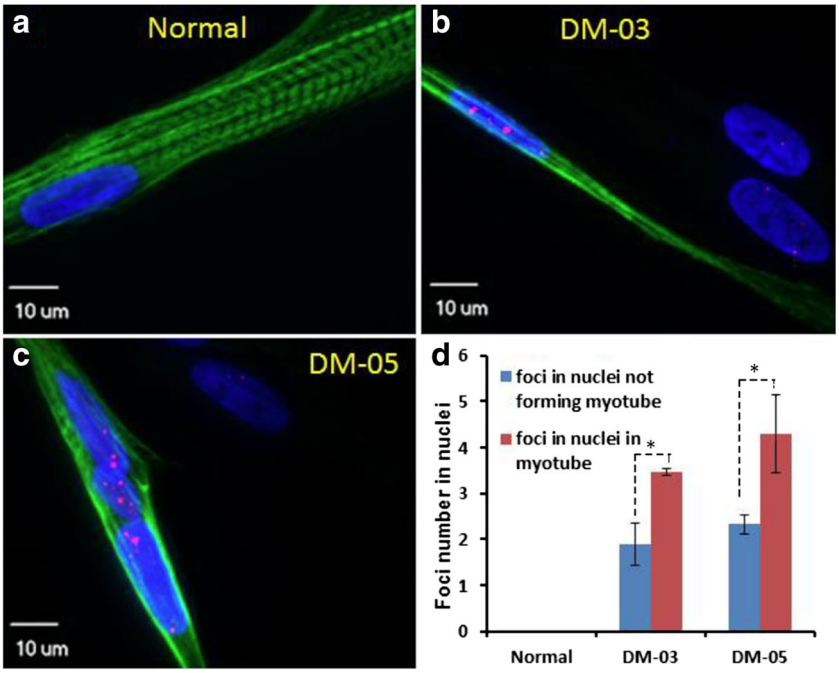

Fig. 5 Intranuclear RNA foci accumulated during early myotube formation. There were no foci in the normal control cells (**a**). Foci accumulated and became bigger and brighter when myoblasts began to express myosin heavy chain in conjunction with fusion (**b**, **c**). Average focus number in the myotube is significantly higher than that in non-myotube forming cells (**d**). $*P < 0.01$

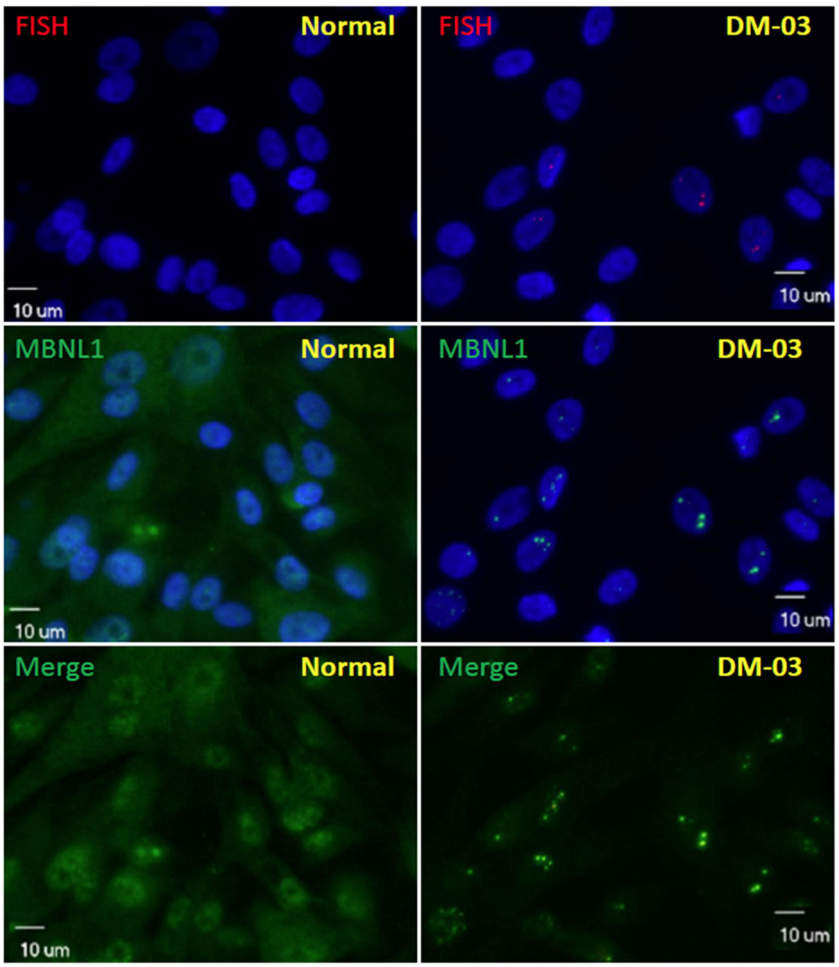

Fig. 6 Co-localization of mutant RNA foci and MBNL1 in DM1 myoblasts. Even though the foci were smaller and fewer compared to differentiated myotubes (Figs. 7 and 9), almost all soluble MBNL1 were sequestered into the mutant RNA foci. Some MBNL1 aggregates had no visible RNA foci. It is unlikely that MBNL1 self-aggregated. When we increased the foci signal, we consistently observed that the foci were associated with MBNL1. In contrast, normal myoblasts had soluble MBNL1 staining in the nuclei, which was best seen when the DAPI channel was turned off (bottom panel)

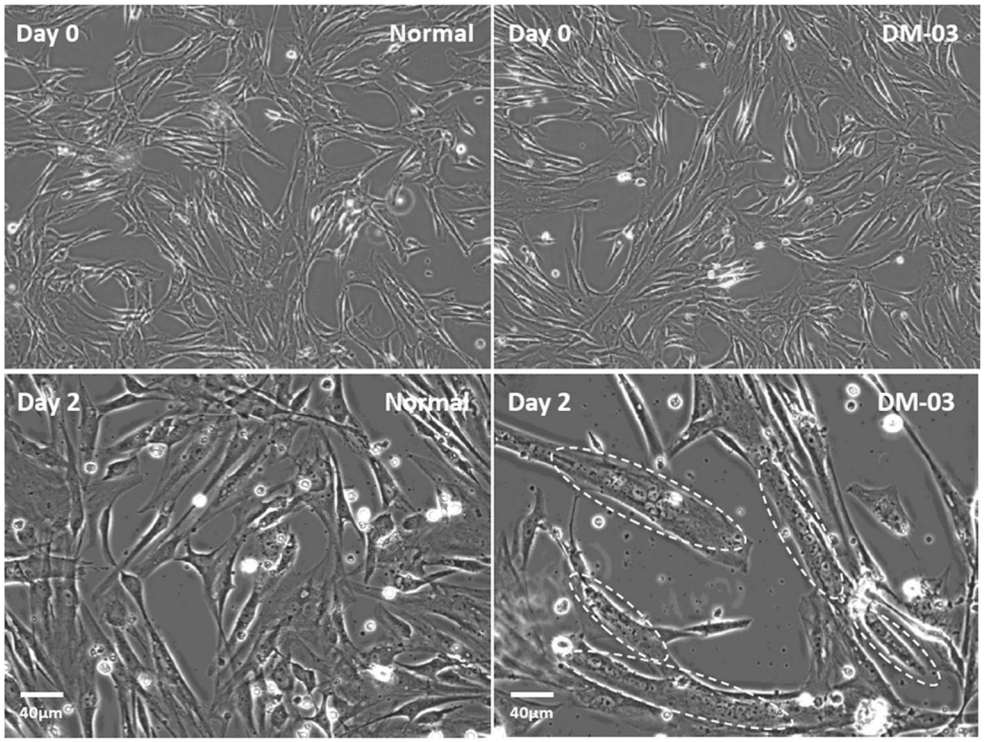

Fig. 7 Nuclear aggregation in early DM1 myotubes observed under phase-contrast microscopy. Both normal and DM1 myocytes were spindle-like and there were no morphology differences. As early as day 2 of the differentiation, DM1 myoblasts fused to become multinucleated myotubes. Nuclei tended to aggregate at the end of the myotubes. In contrast, myotube morphology was not obvious on day 2 of normal myocyte differentiation

studies have found *DMPK* expression increases fivefold 24 h after switching from the proliferative medium (permissive culture condition) to the differentiation medium (non-permissive culture condition), resulting in increased toxic, mutant, intranuclear *DMPK* transcripts [26]. In our study, we also discovered a lower focus load in myoblasts in contrast to myotubes, which may explain why myoblast function is not apparently affected. We conclude that the process of differentiation from satellite cells to myoblasts in vitro is preserved and may not be the cause of muscle wasting in DM1.

Interestingly, we found that DM1 myoblasts proliferated faster than normal myoblasts. We also found the proliferation rate of fibroblasts from DM1 subjects and DM1 iPS-derived neural stem cells is faster than normal control cells of the same passage (our unpublished data). We therefore expect that the higher proliferation rate is intrinsic to DM1 cells, which may

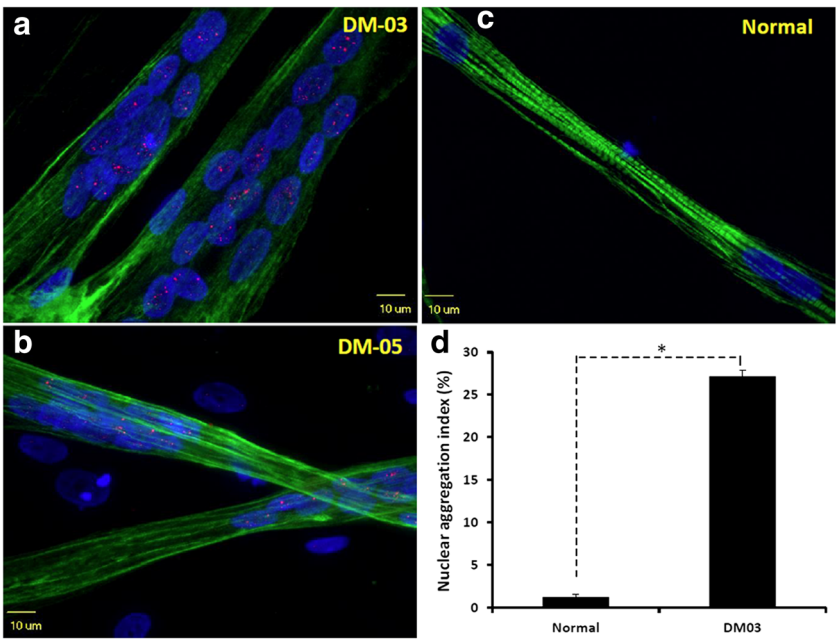

Fig. 8 Increased nuclear aggregation was observed in DM1 myotubes grown in non-permissive culture medium for 5 days. DM1 myotubes contained aggregated, misaligned nuclei with foci accumulation and poorly defined sarcomeres (**a**, **b**). In contrast, nuclei were aligned linearly in normal myotubes which contained well-organized sarcomeres (**c**). Nuclear aggregation index was significantly higher in DM1 myotubes than in the normal control (**d**). $*P < 0.01$

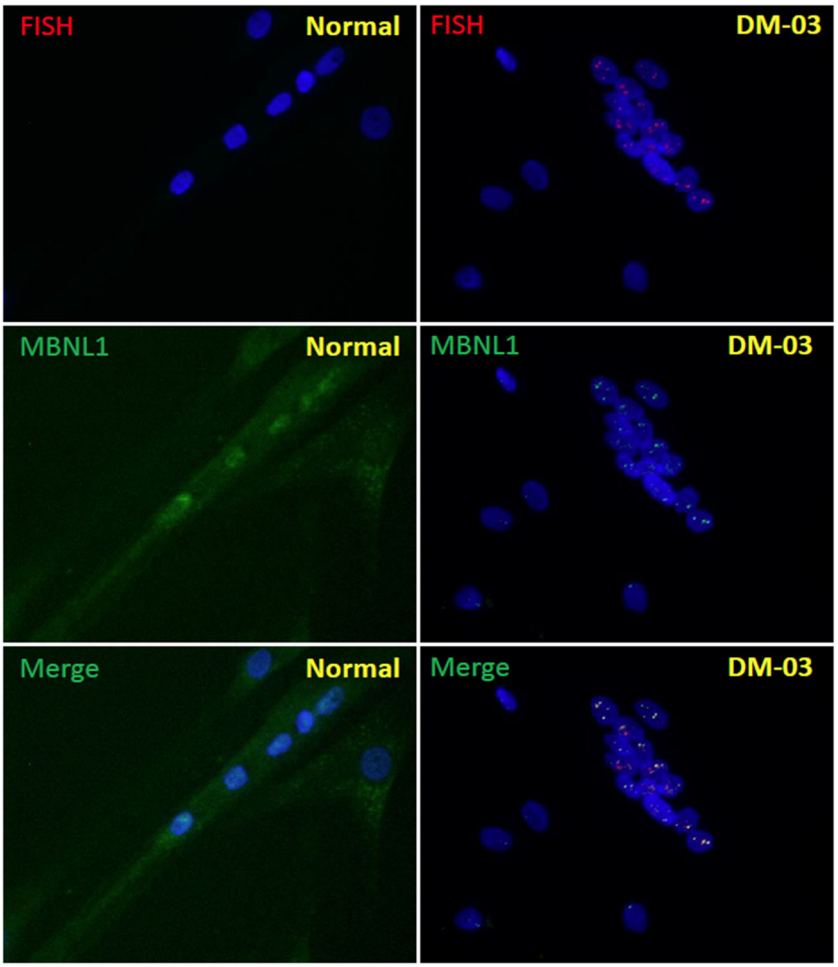

Fig. 9 MBNL1 co-localized with foci in DM1 myotubes. On day 5 of the differentiation, strong co-localization of RNA foci and MBNL1 was observed in aggregated nuclei. The MBNL1 was sequestered into the mutant foci. In contrast, nuclei in normal myoblasts were linearly aligned with soluble MBNL1 staining

predispose the development of cancer in certain tissues. Early studies, and a recent large cohort study, revealed that DM1 patients have a higher risk for developing gynecologic, brain, and thyroid cancer [34–36]. The underlying mechanism and its relationship with the mutation merit investigation, which may give further insight into cancer cell biology.

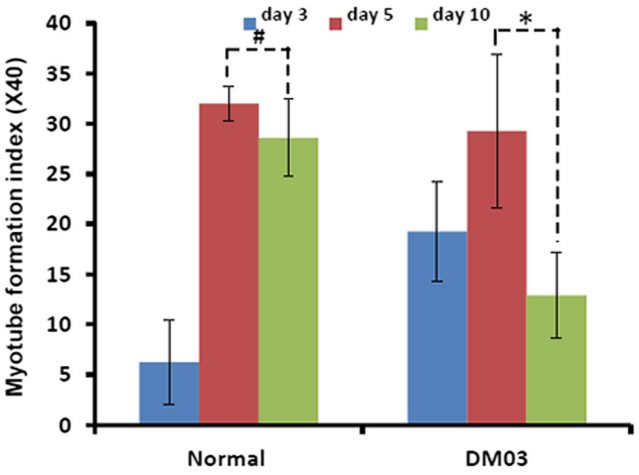

Fig. 10 DM1 (DM03) and normal myotube formation. The myoblast fusion continued until day 5 when it peaked for both normal and DM1 myotubes. DM1 myotubes started degenerating while normal myotubes remained about the same on day 10. $^{\#}P > 0.05$; $^{*}P < 0.01$

Additionally, we found that intranuclear RNA foci accumulated when myoblasts started fusing into myotubes. This could be from the increased expression of the *DMPK* gene [26] or the accumulation of stable mutant transcripts when cells exit the cell cycle, as we observed in neural stem cells [30]. The accumulation of mutant transcripts sequestered MBNL1, depleted soluble MBNL1, and may have produced more toxic effects. This may explain why mature myotubes are more affected than myoblasts.

We also noticed poor nuclear polarization and prominent nuclear aggregation as early as day 2 of the myotube formation in the two DM1 myoblast lines, but not in normal myoblasts. Similar images were also found in studies investigating DM2 myotube formation [37], but the phenomenon has never been systematically evaluated. In our present study, we quantified this phenomenon and compared it to a normal control. We found nuclear aggregation was a common phenomenon at the early stage of myotube formation, which was significantly different from normal myoblasts. We also observed nuclear

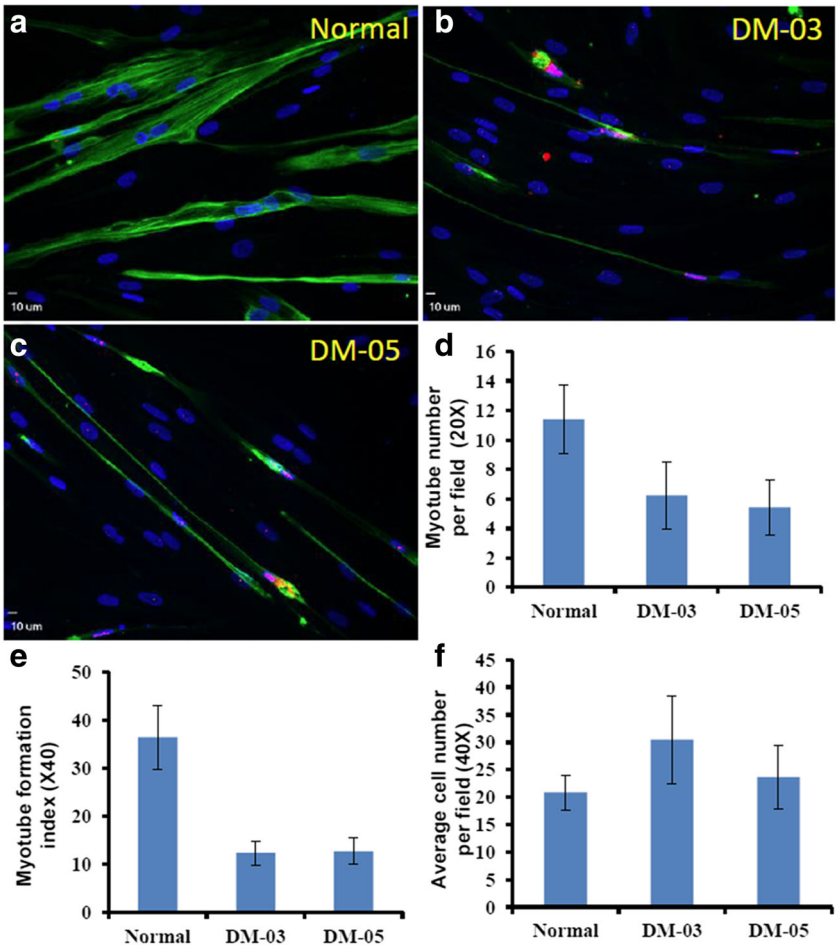

Fig. 11 DM1 myotube degeneration on day 10 of the differentiation. **a**, **b**, **c** Representative field of normal and DM1 myotubes on day 10 of the differentiation. DM1 myotubes were thinner and fewer as shown by MHC staining. **d** Quantification of myotubes per × 20 field showed fewer myotube in DM1. **e** Quantification of myotube formation by the myotube formation index also showed similar findings. **f** The cell density of normal, DM-03, and DM-05 was comparable

aggregation occuring earlier than myotube degeneration. These observations suggest that nuclear aggregation may be used as an early outcome measure to assess effects of therapies in an in vitro culture system. Furthermore, the nuclear aggregation assay is easy to perform. As nuclear aggregation precedes myotube degeneration, nuclear aggregation may be a more sensitive outcome measure than the myotube formation index. Poor nuclear polarization was also found in DM1 myotube formation, and was attributed to poor sensitivity of myoblasts to cues in the extracellular matrix [20]. Further investigation of abnormal nuclear aggregation may shed light onto the pathophysiology of muscular dystrophies.

The skeletal muscle regenerates via proliferation of satellite cell-derived myoblasts that fuse into multinucleated myotubes, which eventually mature into myofibers. This process occurs during embryonic muscle development and in postnatal muscle regeneration in response to external or inherited injury. Traditionally, skeletal muscle regeneration is evaluated in vitro via the myotube formation index. Decreased myotube formation has been reported in both CDM and adult DM1. Early studies reported a malfunction of satellite cell-derived myoblasts in CDM1 [24, 38]. However, a recent study on adult DM1 revealed normal myogenesis but impaired muscle mass maintenance [39]. Our findings revealed no difference with the myotube formation index on day 5 of the differentiation. However, dramatic degeneration was noted on day 10 of the differentiation. These observations are consistent with myotube degeneration rather than altered myogenesis. The degeneration occurs later than abnormal nuclear aggregation; therefore, the myotube formation index may be utilized as a late outcome measure for functional analyses of DM1 myoblast following treatment. For myotube formation analysis, we recommend looking for changes of myotube formation starting on day 5 of the differentiation.

The mechanism of myotube degeneration in DM1 remains unclear. In a recent report using myoblasts generated from an adult DM1 muscle biopsy, the authors reported normal myogenesis, but considerable myotube loss and atrophy in DM1 myotubes differentiated for 15 days, which was attributed to apoptosis [39]. In our study, we found equal cell density during DM1 myotube degeneration on day 10 of the differentiation. Thus, apoptosis may not be the only reason for myotube formation degeneration. This is also supported by the fact that atrophied muscle fibers contain nuclear clumps in the biopsied tissue [24]. We propose the degeneration of myofibrils may launch the starting process of muscle wasting.

There are limitations for this study. This study was done on only two DM1 cases. Ideally, 4 or 5 cases would be ideal in order to do a statistical analysis.

Conclusions

We concluded that early abnormal nuclear aggregation and late myotube degeneration offer easy and sensitive outcome measures to assess effects of therapies for DM1 in vitro.

Acknowledgements Research reported in this publication was supported by the NIH/NIAMS grant K08 AR064836 to G.X. mentored by Maury S. Swanson, Tetsuo Ashizawa, Laura Ranum, Naohiro Terada, and SH Subramony at the University of Florida and Fernando Valenzuela in University of New Mexico and by startup funds from the Office of Research at the Health Science Center of University of New Mexico. We would like to thank Alexis K Hall for proofreading, as well as submitting suggestions on the manuscript.

Compliance with ethical standards

The present study involved research on healthy and DM1 subjects who provided their informed consent to participate.

Conflict of interest The authors declare that they have no conflict of interest.

References

1. Harper P (2001) Myotonic dystrophy, 3rd edn. WB Saunders, London
2. Romeo V (2012) Myotonic dystrophy type 1 or Steinert's disease. Adv Exp Med Biol 724:239–257. https://doi.org/10.1007/978-1-4614-0653-2_18
3. Campbell C, Levin S, Siu VM, Venance S, Jacob P (2013) Congenital myotonic dystrophy: Canadian population-based surveillance study. J Pediatr 163(1):120–125 e121–123. https://doi.org/10.1016/j.jpeds.2012.12.070
4. Fu YH, Pizzuti A, Fenwick RG Jr, King J, Rajnarayan S, Dunne PW, Dubel J, Nasser GA, Ashizawa T, de Jong P et al (1992) An unstable triplet repeat in a gene related to myotonic muscular dystrophy. Science 255(5049):1256–1258
5. Ashizawa T, Sarkar PS (2011) Myotonic dystrophy types 1 and 2. Handb Clin Neurol 101:193–237. https://doi.org/10.1016/B978-0-08-045031-5.00015-3
6. Ranum LP, Cooper TA (2006) RNA-mediated neuromuscular disorders. Annu Rev Neurosci 29:259–277. https://doi.org/10.1146/annurev.neuro.29.051605.113014
7. Lee JE, Cooper TA (2009) Pathogenic mechanisms of myotonic dystrophy. Biochem Soc Trans 37(Pt 6):1281–1286. https://doi.org/10.1042/BST0371281
8. Gomes-Pereira M, Cooper TA, Gourdon G (2011) Myotonic dystrophy mouse models: towards rational therapy development. Trends Mol Med 17(9):506–517. https://doi.org/10.1016/j.molmed.2011.05.004
9. Chau A, Kalsotra A (2015) Developmental insights into the pathology of and therapeutic strategies for DM1: back to the basics. Dev Dyn 244(3):377–390. https://doi.org/10.1002/dvdy.24240
10. Meola G, Cardani R (2015) Myotonic dystrophies: an update on clinical aspects, genetic, pathology, and molecular pathomechanisms. Biochim Biophys Acta 1852(4):594–606. https://doi.org/10.1016/j.bbadis.2014.05.019
11. Takahashi K, Tanabe K, Ohnuki M, Narita M, Ichisaka T, Tomoda K, Yamanaka S (2007) Induction of pluripotent stem cells from adult human fibroblasts by defined factors. Cell 131(5):861–872
12. Yu J, Vodyanik MA, Smuga-Otto K, Antosiewicz-Bourget J, Frane JL, Tian S, Nie J, Jonsdottir GA, Ruotti V, Stewart R, Slukvin II, Thomson JA (2007) Induced pluripotent stem cell lines derived from human somatic cells. Science 318(5858):1917–1920
13. Meissner A, Wernig M, Jaenisch R (2007) Direct reprogramming of genetically unmodified fibroblasts into pluripotent stem cells. Nat Biotechnol 25(10):1177–1181
14. Maffioletti SM, Gerli MF, Ragazzi M, Dastidar S, Benedetti S, Loperfido M, VandenDriessche T, Chuah MK, Tedesco FS (2015) Efficient derivation and inducible differentiation of expandable skeletal myogenic cells from human ES and patient-specific iPS cells. Nat Protoc 10(7):941–958. https://doi.org/10.1038/nprot.2015.057
15. Darabi R, Arpke RW, Irion S, Dimos JT, Grskovic M, Kyba M, Perlingeiro RC (2012) Human ES- and iPS-derived myogenic progenitors restore DYSTROPHIN and improve contractility upon transplantation in dystrophic mice. Cell Stem Cell 10(5):610–619. https://doi.org/10.1016/j.stem.2012.02.015
16. Darabi R, Perlingeiro RC (2016) Derivation of skeletal myogenic precursors from human pluripotent stem cells using conditional expression of PAX7. Methods Mol Biol 1357:423–439. https://doi.org/10.1007/7651_2014_134
17. Chal J, Al Tanoury Z, Hestin M, Gobert B, Aivio S, Hick A, Cherrier T, Nesmith AP, Parker KK, Pourquie O (2016) Generation of human muscle fibers and satellite-like cells from human pluripotent stem cells in vitro. Nat Protoc 11(10):1833–1850. https://doi.org/10.1038/nprot.2016.110
18. Gao Y, Guo X, Santostefano K, Wang Y, Reid T, Zeng D, Terada N, Ashizawa T, Xia G (2016) Genome therapy of myotonic dystrophy type 1 iPS cells for development of autologous stem cell therapy. Mol Ther 24(8):1378–1387. https://doi.org/10.1038/mt.2016.97
19. Wang Y, Hao L, Wang H, Santostefano K, Thapa A, Cleary J, Li H, Guo X, Terada N, Ashizawa T, Xia G (2018) Therapeutic genome editing for myotonic dystrophy type 1 using CRISPR/Cas9. Mol Ther 26:2617–2630. https://doi.org/10.1016/j.ymthe.2018.09.003
20. Nesmith AP, Wagner MA, Pasqualini FS, O'Connor BB, Pincus MJ, August PR, Parker KK (2016) A human in vitro model of Duchenne muscular dystrophy muscle formation and contractility. J Cell Biol 215(1):47–56. https://doi.org/10.1083/jcb.201603111
21. Sarnat HB, Silbert SW (1976) Maturational arrest of fetal muscle in neonatal myotonic dystrophy. A pathologic study of four cases. Arch Neurol 33(7):466–474
22. Sahgal V, Bernes S, Sahgal S, Lischwey C, Subramani V (1983) Skeletal muscle in preterm infants with congenital myotonic dystrophy. Morphologic and histochemical study. J Neurol Sci 59(1):47–55
23. Farkas-Bargeton E, Barbet JP, Dancea S, Wehrle R, Checouri A, Dulac O (1988) Immaturity of muscle fibers in the congenital form of myotonic dystrophy: its consequences and its origin. J Neurol Sci 83(2–3):145–159
24. Thornell LE, Lindstom M, Renault V, Klein A, Mouly V, Ansved T, Butler-Browne G, Furling D (2009) Satellite cell dysfunction contributes to the progressive muscle atrophy in myotonic dystrophy type 1. Neuropathol Appl Neurobiol 35(6):603–613. https://doi.org/10.1111/j.1365-2990.2009.01014.x

25. Furling D, Coiffier L, Mouly V, Barbet JP, St Guily JL, Taneja K, Gourdon G, Junien C, Butler-Browne GS (2001) Defective satellite cells in congenital myotonic dystrophy. Hum Mol Genet 10(19): 2079–2087
26. Furling D, Lemieux D, Taneja K, Puymirat J (2001) Decreased levels of myotonic dystrophy protein kinase (DMPK) and delayed differentiation in human myotonic dystrophy myoblasts. Neuromuscul Disord 11(8):728–735
27. Furling D, Doucet G, Langlois MA, Timchenko L, Belanger E, Cossette L, Puymirat J (2003) Viral vector producing antisense RNA restores myotonic dystrophy myoblast functions. Gene Ther 10(9):795–802. https://doi.org/10.1038/sj.gt.3301955
28. Xia G, Santostefano KE, Goodwin M, Liu J, Subramony SH, Swanson MS, Terada N, Ashizawa T (2013) Generation of neural cells from DM1 induced pluripotent stem cells as cellular model for the study of central nervous system neuropathogenesis. Cell Rep 15(2):166–177. https://doi.org/10.1089/cell.2012.0086
29. Xia G, Gao Y, Jin S, Subramony SH, Terada N, Ranum LP, Swanson MS, Ashizawa T (2015) Genome modification leads to phenotype reversal in human myotonic dystrophy type 1 induced pluripotent stem cell-derived neural stem cells. Stem Cells 33(6): 1829–1838. https://doi.org/10.1002/stem.1970
30. Xia G, Ashizawa T (2015) Dynamic changes of nuclear RNA foci in proliferating DM1 cells. Histochem Cell Biol 143:557–564. https://doi.org/10.1007/s00418-015-1315-5
31. Murata-Hori M, Tatsuka M, Wang YL (2002) Probing the dynamics and functions of aurora B kinase in living cells during mitosis and cytokinesis. Mol Biol Cell 13(4):1099–1108. https://doi.org/10.1091/mbc.01-09-0467
32. McKinnell IW, Parise G, Rudnicki MA (2005) Muscle stem cells and regenerative myogenesis. Curr Top Dev Biol 71:113–130. https://doi.org/10.1016/S0070-2153(05)71004-8
33. Dumont NA, Wang YX, von Maltzahn J, Pasut A, Bentzinger CF, Brun CE, Rudnicki MA (2015) Dystrophin expression in muscle stem cells regulates their polarity and asymmetric division. Nat Med 21(12):1455–1463. https://doi.org/10.1038/nm.3990
34. Gadalla SM, Lund M, Pfeiffer RM, Gortz S, Mueller CM, Moxley RT 3rd, Kristinsson SY, Bjorkholm M, Shebl FM, Hilbert JE, Landgren O, Wohlfahrt J, Melbye M, Greene MH (2011) Cancer risk among patients with myotonic muscular dystrophy. JAMA 306(22):2480–2486. https://doi.org/10.1001/jama.2011.1796
35. Fernandez-Torron R, Garcia-Puga M, Emparanza JI, Maneiro M, Cobo AM, Poza JJ, Espinal JB, Zulaica M, Ruiz I, Martorell L, Otaegui D, Matheu A, Lopez de Munain A (2016) Cancer risk in DM1 is sex-related and linked to miRNA-200/141 downregulation. Neurology 87(12):1250–1257. https://doi.org/10.1212/WNL.0000000000003124
36. Win AK, Perattur PG, Pulido JS, Pulido CM, Lindor NM (2012) Increased cancer risks in myotonic dystrophy. Mayo Clin Proc 87(2):130–135. https://doi.org/10.1016/j.mayocp.2011.09.005
37. Schoser BG, Kress W, Walter MC, Halliger-Keller B, Lochmuller H, Ricker K (2004) Homozygosity for CCTG mutation in myotonic dystrophy type 2. Brain 127(Pt 8):1868–1877. https://doi.org/10.1093/brain/awh210
38. Timchenko NA, Iakova P, Cai ZJ, Smith JR, Timchenko LT (2001) Molecular basis for impaired muscle differentiation in myotonic dystrophy. Mol Cell Biol 21(20):6927–6938. https://doi.org/10.1128/MCB.21.20.6927-6938.2001
39. Loro E, Rinaldi F, Malena A, Masiero E, Novelli G, Angelini C, Romeo V, Sandri M, Botta A, Vergani L (2010) Normal myogenesis and increased apoptosis in myotonic dystrophy type-1 muscle cells. Cell Death Differ 17(8):1315–1324. https://doi.org/10.1038/cdd.2010.33